Università di Padova - Dipartimento di Ingegneria dell'Informazione,
via Gradenigo 6/b 35131 Padova (Italy)
Tel. +39.049.827.7600
Fax +39.049.827.7699

TID and SEE Report on

Micron MT29F32G08CBACA

Multi-Level-Cell NAND Flash Memory

Authors: Marta Bagatin, Simone Gerardin, Alessandro Paccagnella, Università di Padova

The work described in this report was done under
ESA Contract 4000103347/11/NL/PA
"Studies of radiation effects in new generation of non-volatile memories"

Technical officer: Véronique Ferlet-Cavrois, ESA ESTEC, TEC-QEC

v1.0
Date: March 2013

TABLE OF CONTENTS

FIGURES

TABLES

1 Introduction

Under ESA Contract 4000103347/11/NL/PA “Studies of Radiation Effects in New Generation of Non-volatile Memories”, we evaluated Total Ionizing Dose (TID) and Single Event Effects (SEE) in Micron MT29F32G08CBACA Multi-Level-Cell Flash Memories.

NAND Flash memories are based on Floating Gate (FG) cells and they are currently the leading technology in the market of large-size non-volatile memories. Multi-Level Cell (MLC) Flash memories store more than one memory bit in each FG cell.

2 Applicable and Reference Documents

- ESCC22900 Total Ionizing Dose (TID) Testing
- ESCC25100 Single Event Effects (SEE) Testing
- Micron MT29F32G08CBACA Multi-Level-Cell Flash Memory datasheet

3 Tested Devices

For this work we used two-bit-per-cell 32-Gbit MLC NAND Flash memories manufactured by Micron with a 25-nm feature size. The details of the tested samples are reported in **Table 1**.

The plastic package of the devices to be irradiated with heavy ions and x rays was etched with an acid attack.

Internal reference number	MG7 MG8 MG9 MG10 MG18 MG19 MG21 MG23 MG43 MG45	MG38 MG39 MG40	MG48 MG49	MG1
Part number	MT29F32G08CBACA	MT29F32G08CBACA	MT29F32G08CBACA	MT29F32G08CBACA
Supply voltage	2.7V-3.6V	2.7V-3.6V	2.7V-3.6V	2.7V-3.6V
Density	32 Gbit	32 Gbit	32 Gbit	32 Gbit
ECC requirements	24-bit ECC per 1080 bytes of data	24-bit ECC per 1080 bytes of data	24-bit ECC per 1080 bytes of data	24-bit ECC per 1080 bytes of data
Package	48-pin TSOP	48-pin TSOP, decapped	48-pin TSOP	48-pin TSOP
Operating temperature	0°C to +70°C	0°C to +70°C	0°C to +70°C	0°C to +70°C
Lot code	Unknown	Unknown	Unknown	Unknown
Package markings	III2 I-2 29F32G08CBACA WP C	III2 I-2 29F32G08CBACAW P C	III2 I-2 29F32G08CBACA WP C	III2 I-2 29F32G08CBACA WP C
Die markings	n.a.	n.a. (corners of the die are not exposed)	n.a.	n.a.
Test	TID	Heavy ions	Protons	Reference

Table 1: Details of the MLC NAND memories used for this work.

4 Total Ionizing Dose (TID) Tests

4.1 Experimental Conditions

Irradiations were performed using the Co60 source at ESA-ESTEC (Noordwijk, The Netherlands). Two TID test campaigns were performed, one in June 2011 and the other one in December 2011. A dose rate of about 1.4 rad(Si)/s was used.

In addition, a further test campaign was performed using a 10-keV x-ray probe station at the Laboratori Nazionali di Legnaro, LNL (Padova, Italy). A dose rate of 10 rad(Si)/s has been used.

The main experimental details concerning TID tests are summarized in **Table 2**.

Run	Start	Stop	Source	Dose rate(Si) [rad/s]	Dose(Si) [krad]	DUTs	Operating conditions
2_A	28/06/2011 10.42	29/06/2011 11.24	ESTEC Co^{60}	1.3775	122.5	MG18	High-duty cycle
4_A	29/06/2011 19.07	30/06/2011 11.52	ESTEC Co^{60}	1.3785	83.2	MG19	Low-duty cycle
6_A	30/06/2011 15.05	30/06/2011 15.23	ESTEC Co^{60}	1.373	1.5	MG21	High-duty cycle
7_A	30/06/2011 15.25	01/07/2011 9.14	ESTEC Co^{60}	1.37575	88.2	MG21	High-duty cycle
12_A	01/07/2011 16.24	01/07/2011 19.08	ESTEC Co^{60}	1.3745	13.5	MG43	Low-duty cycle
13_A	01/07/2011 19.14	04/07/2011 9.18	ESTEC Co^{60}	1.3735	306.4	MG43	Low-duty cycle
2_B	03/12/2011 12.56	04/12/2011 12.16	ESTEC Co^{60}	1.419	119.2	MG7	Unbiased
3_B	04/12/2011 12.49	05/12/2011 15.34	ESTEC Co^{60}	1.418	136.5	MG8-MG9	Unbiased
4_B	05/12/2011 15.59	06/12/2011 11.01	ESTEC Co^{60}	1.4185	97.1	MG10	High-duty cycle
1_C	22/02/2012 12.49	22/02/2012 16.51	LNL x rays	10	143.0	MG22	High-duty cycle
2_C	27/02/2012 14.25	27/02/2012 17.29	LNL x rays	10	100.5	MG24	High-duty cycle

Table 2: Gamma TID runs performed at ESA/ESTEC Co-60 source and x-ray tests performed at the Laboratori Nazionali di Legnaro (LNL).

The used test setup consists of an FPGA motherboard controlled by a host PC and a daughterboard with an open-top socket, where the Device Under Test (DUT) is placed. The connection between the two boards is implemented through a couple of high-speed connectors. The supply current drawn by the memory under test is constantly monitored through a PC-controlled multimeter and stored on log. A PC-controlled power supply is used to supply the DUT.

A schematic illustration of the irradiation setup is shown in **Fig. 1**. The FPGA controlling board is protected from gamma rays through proper shielding bricks available at the ESTEC Co60 facility.

During the TID tests, 2 Gbits for each memory were exercised with Erase/Read/Program/Read (E/R/P/R) loops, whereas another portion (again 2 Gbit) was kept in retention mode and periodically read.

Different operating conditions were used during the tests:

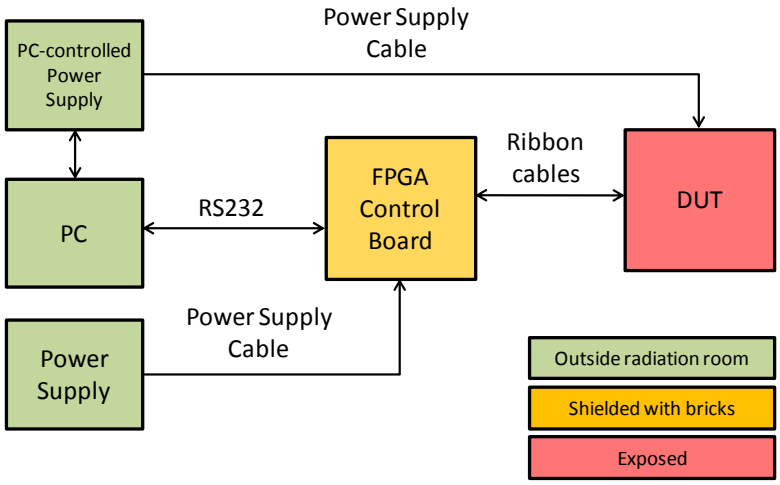

Figure 1: Irradiation setup.

- **High-duty cycle**, with continuous Erase/Program operations to maximize the use of cells, charge pumps, and control circuitry. In particular the following sequence of operations was implemented:
  1 10 E/R/P/R loops with pseudo-random patterns (duration ~ 170 s)
  2 Read of the cells kept in retention (few s)
  3 Go to 1 if no failure
- **Low-duty cycle**, with the memory performing Erase/Program operation less than 0.2 % of the time. In particular the following sequence of operations was implemented:
  1 10 E/R/P/R loops with pseudo-random patterns (duration ~ 170 s)
  2 Read of the cells kept in retention (few s)
  3 Refresh of cells in retention
  4 Memory in standby for 25 minutes
  5 Go to 1 if no failure
- **Unbiased**: same as for low-duty cycle, except for 3:
  3 Memory unbiased for 25 minutes

For low-duty cycle irradiations the cells kept in retention mode were refreshed after each read, whereas they were not refreshed during high-duty cycle and unbiased exposures.

After each erase, program, and read operation, different parameters/signals were monitored during irradiation:

- The Status Register (SR) which signals if erase and program operations have been successfully performed.
- The Ready/Busy (RB), which is a device output that indicates if the memory is busy or is ready to accept new commands. For instance, during a program operation the RB signal is active (low); as soon as the operation is completed, the RB becomes inactive (high).

In detail:

- After erase operations we logged:
  - SR, to detect erase fails;
  - RB low time, to measure the erase time;
  -
- After each program operation we logged:
  - SR, to detect program fails;
  - RB low time, to measure the program time;

- After each read operation we logged:
  - RB low time, to measure the read time;
  - Number and location of errors.

Finally, for cells kept in retention during dynamic tests, we logged the number and location of errors.

4.2 Experimental Results

4.2.1 Retention

Fig. 2 shows the error build-up in the FG cells kept in retention mode as a function of dose, for memories irradiated with high-duty cycle, low-duty cycle, and unbiased conditions.

It is worth to remark that these samples show intrinsic errors after program (about 2000-3000 in the set of cells we are studying), and require the use of Error Correction Codes (ECC) even at sea level.

An increase in the number of retention errors occurs between 20 and 30 krad(Si) in high-duty cycle and in unbiased samples, whereas the increase in retention errors takes place between 50 and 55 krad(Si) in low-duty cycle devices, thanks to the refresh operation.

4.2.2 Erase/Read/Program/Read Loops

Fig. 3 plots the number of erase fails as a function of dose, for samples irradiated in high-duty cycle, low-duty cycle, and unbiased conditions. This kind of errors is detected when the SR signals that an erase operation has not been successfully carried out. Erase errors appear between 50 and 75 krad(Si), depending on the duty cycle.

Fig. 4 shows the block erase time as a function of dose, for samples irradiated in high-duty cycle, low-duty cycle, and unbiased conditions. As seen, the time to erase either increases or decreases at about the same doses at which the erase operation fails (see Fig. 3). It is worth to note that the variation of the block erase time in a reference non-irradiated sample subject to the same high-duty cycle loop as the irradiated samples is negligible.

Fig. 5 shows the number of errors detected in the read after erase, for samples irradiated in high-duty cycle, low-duty cycle, and unbiased conditions. The errors start to increase between 60 and 85 krad(Si).

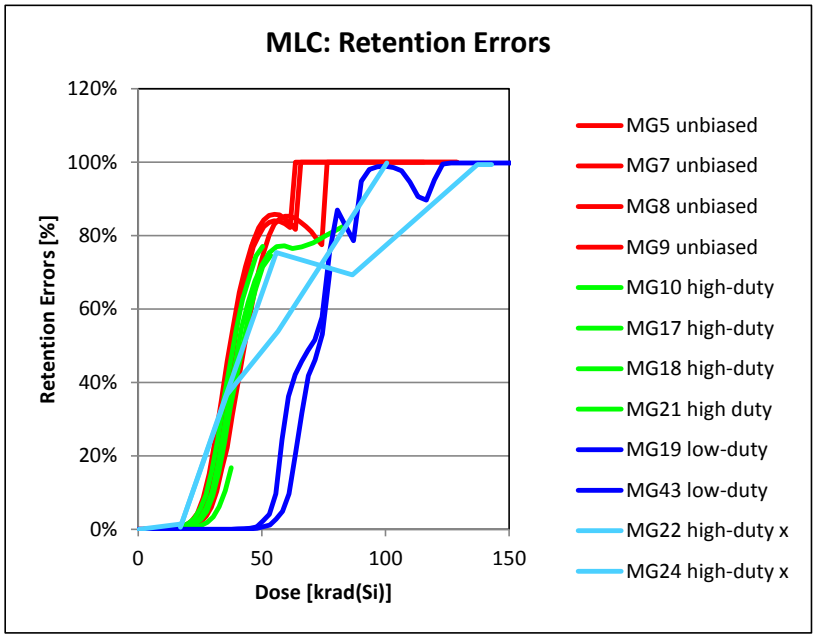

Figure 2: Byte errors in retention cells as a function of dose (refresh is performed in low-duty cycle irradiation only).

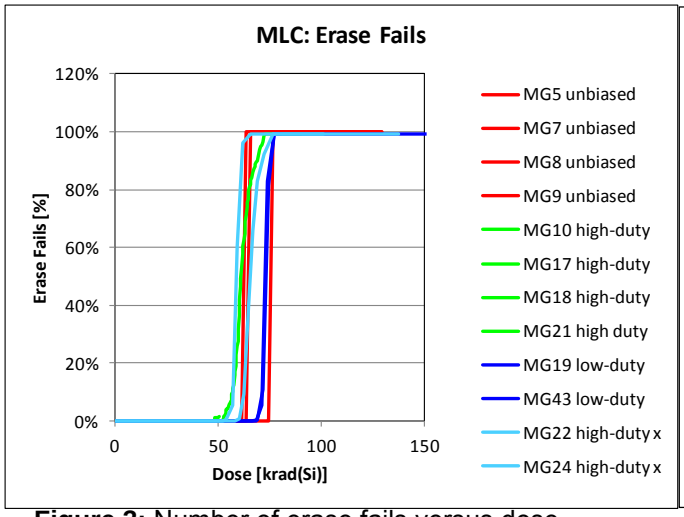

Figure 3: Number of erase fails versus dose.

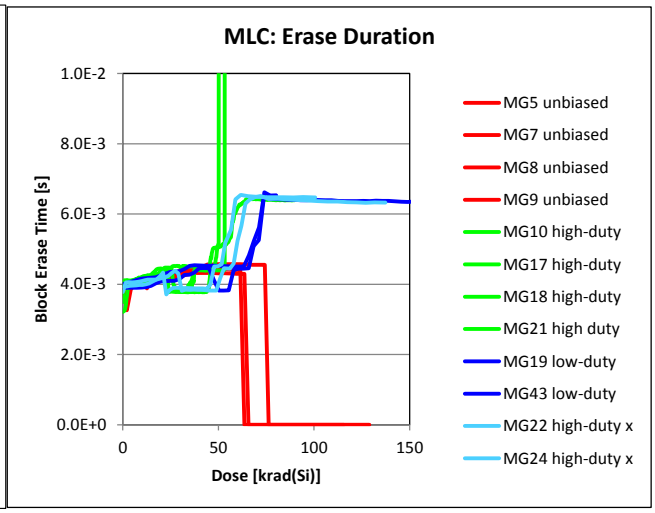

Figure 4: Block erase time versus dose.

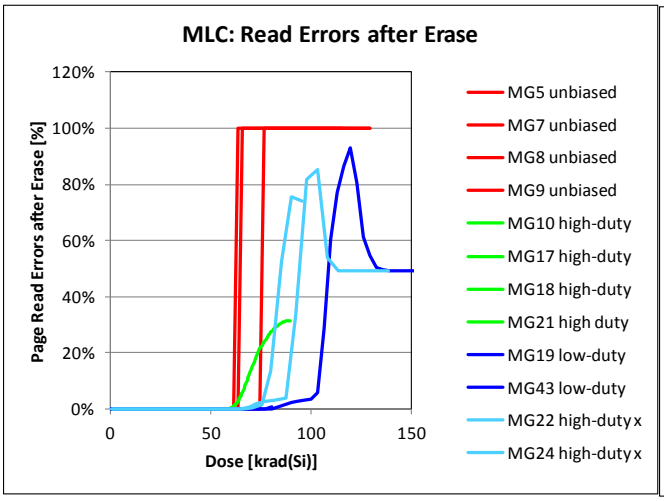

Figure 5: Number of errors in the read after erase versus dose.

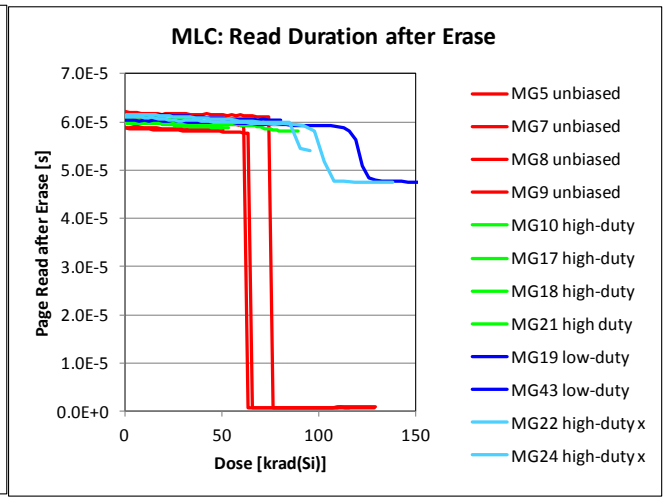

Figure 6: Page read time (after erase) versus dose.

Fig. 6 shows the page read time (after erase) as a function of dose, for samples irradiated in high-duty cycle, low-duty cycle, and unbiased conditions. It is worth to note that the variation of the page read time in a reference non-irradiated sample subject to the same high-duty cycle loop as the irradiated samples is negligible.

Fig. 7 depicts the number of page program errors as a function of dose, for samples irradiated in high-duty cycle, low-duty cycle, and unbiased conditions. This kind of errors occurs when the SR signals that a program operation has not been successfully carried out. Program errors appear between 65 and 75 krad(Si) in all devices, no matter how they are operated during exposure.

Fig. 8 illustrates the page program time as a function of dose, for samples irradiated in high-duty cycle, low-duty cycle, and unbiased conditions. As seen, after a slight increase in the program time, either an increase or a decrease of the program time takes place at the same doses at which the page program fails (see Fig. 7). It is worth to note that the variation of the page program time in a reference non-irradiated sample subject to the same high-duty cycle loop as the irradiated samples is negligible.

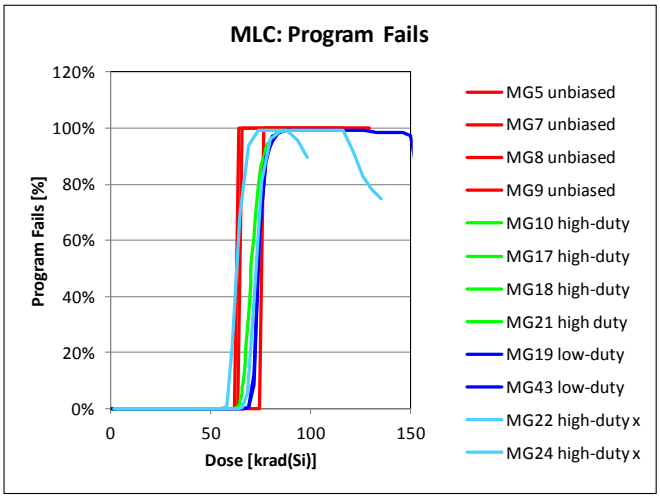

Figure 7: Number of page program fails versus dose.

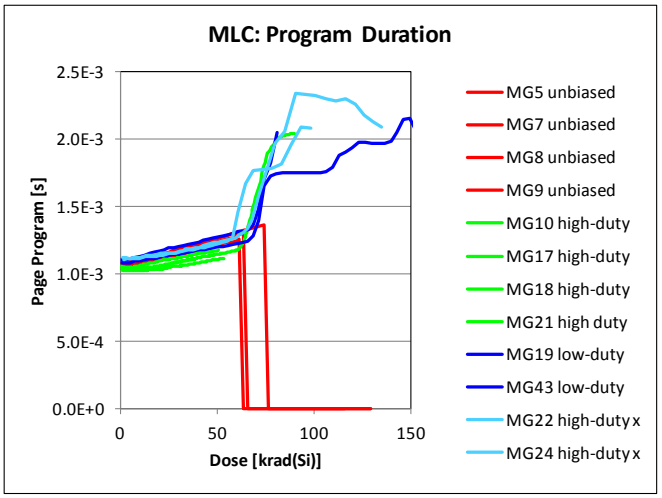

Figure 8: Page program time versus dose.

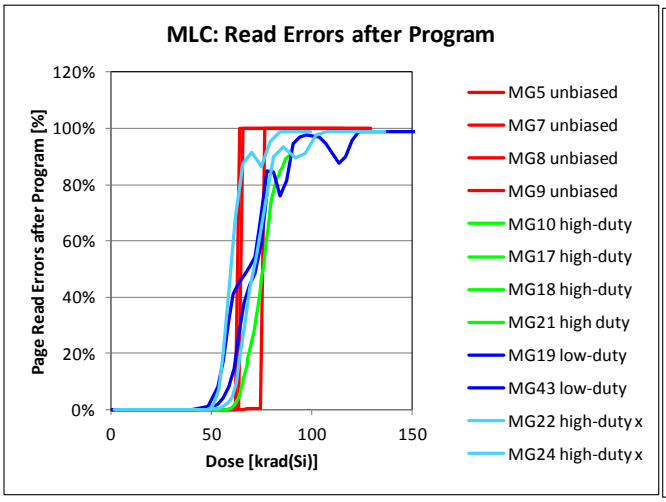

Figure 9: Number of errors in the read after program versus dose.

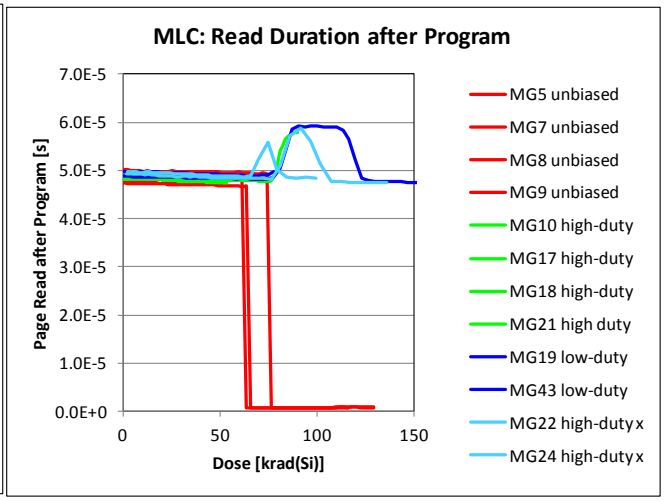

Figure 10: Page read time (after program) versus dose.

Fig. 9 shows the number of errors detected in the read after program, for samples irradiated in high-duty cycle, low-duty cycle, and unbiased conditions. An increase in the errors after program occurs after 50 krad(Si).

Fig. 10 shows the page read time (after program) as a function of dose, for samples irradiated in high-duty cycle, low-duty cycle, and unbiased conditions. Either an abrupt increase or decrease of the page read time is observed at the same doses at which the page read errors increase as well (see Fig. 9). It is worth to note that the variation of the page read time in the reference non-irradiated sample subject to the same high-duty cycle loop as the irradiated samples is negligible.

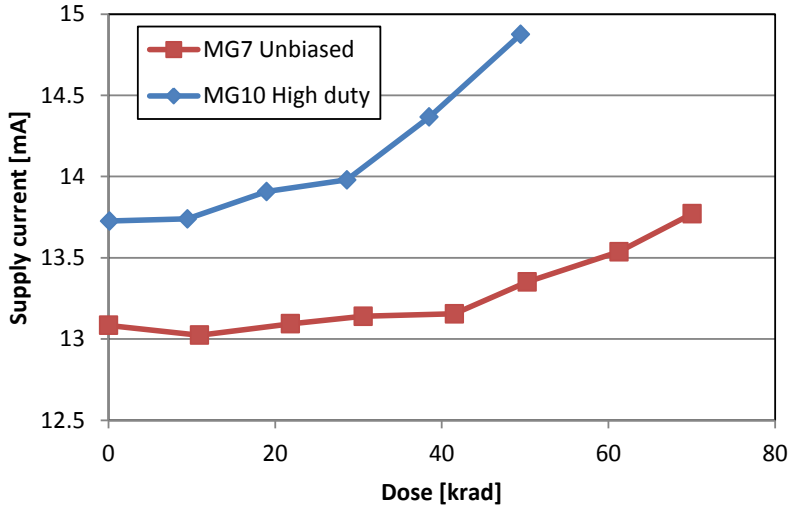

Figure 11: Program current as a function of dose during irradiation.

4.2.3 Supply current during Irradiation

Fig. 11 shows the program current as a function of dose. A moderate increase is visible, irrespective of the bias conditions.

4.2.4 Failure Doses: Summary

Fig. 12 summarizes the average failure doses for erase errors, program errors, check after erase errors, check after program errors, and retention errors, for devices operated in the three tested conditions. For both erase and program, the higher the duty cycle, the lower the failure dose. On the other hand, retention errors appear at comparable doses, no matter if the device is kept unbiased for most of the time or it is operated at high-duty cycle. As shown before, refresh can increase the failure dose for cells kept in retention.

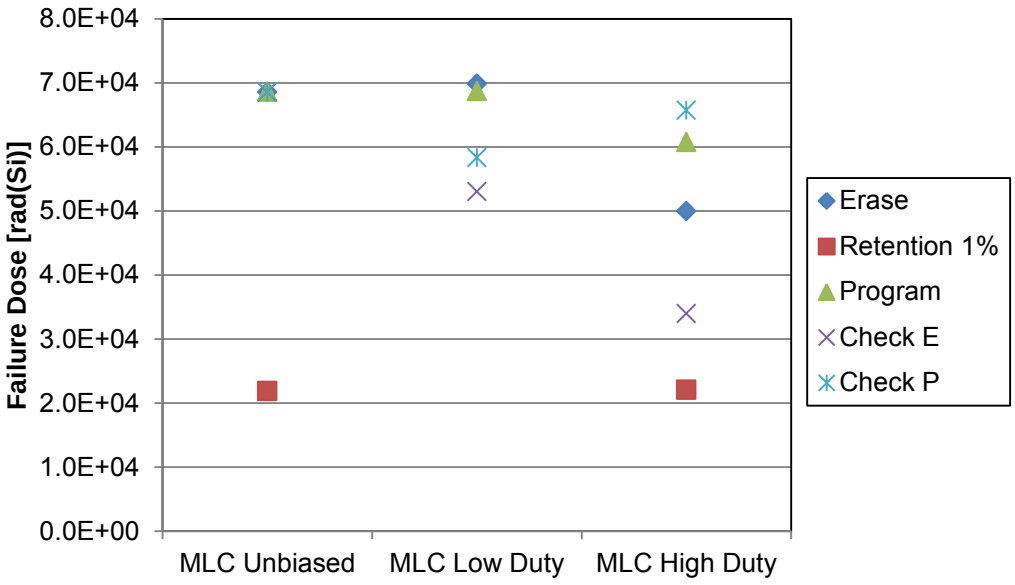

Figure 12: Failure doses for erase, program, check after erase, check after program, and retention errors (1% of the irradiated cells).

4.2.5 Post-radiation Annealing

After the gamma exposure, samples MG17, MG18, MG19, MG21, and MG43 were stored for 1 week at room temperature with shorted pins. Then the memories were tested: no recovery was observed. Afterwards, the same samples were baked at 100°C for 1 week at the University of Padova, with shorted pins. Again no recovery was observed.

All the samples were stored at room temperature after the exposure and/or annealing and were tested (read/erase/program) again about 21 months after irradiation (MG17, MG18, MG19, MG21, MG43) or about 15 months after irradiation (MG5, MG7, MG8, MG9, MG10). No functionality recovery was observed.

It is worth to note that the TID exposures were not stopped immediately after failure, but continued until access to the facility was possible (e.g. if a failure occurred during the night, the exposure was actually stopped the morning after). As a result, the doses after which the samples were stored at room temperature may be significantly larger than the failure doses indicated above.

5 Single Event Effects (SEE) Tests

5.1 Experimental conditions

Heavy-ion irradiations have been performed at the Heavy-Ion Facility (HIF) in Louvain-la-Neuve, Belgium, using the beams listed in **Table 3**.

Ion Species	Cocktail	Energy [MeV]	EFF. LET [MeV cm^2/mg]	Angle [°]	Memory condition	Monitored effects
N	High LET	60	3.30	0	E/R/P/R	SEFIs
Ne	High LET	78	6.40	0	E/R/P/R	SEFIs
Ar	High LET	151	15.90	0	Unbiased	FG errors
			15.90	0	E/R/P/R	SEFIs
			15.90	0	Standby sel.	Destructive events
Kr	High LET	305	40.40	0	E/R/P/R	SEFIs
			40.40	0	Standby sel.	Destructive events

Ion Species	Cocktail	Energy [MeV]	EFF. LET [MeV cm^2/mg]	Angle [°]	Memory condition	Monitored effects
Ne	High energy	235	3	0	Unbiased	FG errors
			3.11	15	Unbiased	FG errors
			3.46	30	Unbiased	FG errors
			4.24	45	Unbiased	FG errors
			6	60	Unbiased	FG errors
Ar	High energy	372	10.2	0	Unbiased	FG errors
			10.56	15	Unbiased	FG errors
			11.78	30	Unbiased	FG errors
			14.42	45	Unbiased	FG errors
			20.4	60	Unbiased	FG errors
Ni	High energy	567	20.4	0	Unbiased	FG errors
			21.12	15	Unbiased	FG errors
			23.56	30	Unbiased	FG errors
			28.85	45	Unbiased	FG errors
			40.8	60	Unbiased	FG errors
Kr	High energy	756	32.6	0	Unbiased	FG errors
			33.75	15	Unbiased	FG errors
			37.64	30	Unbiased	FG errors
			46.1	45	Unbiased	FG errors
			65.2	60	Unbiased	FG errors

Table 3: Heavy-ion beams and test conditions used at HIF.

Ion Species	Energy [MeV]	Memory condition	Monitored effects
proton	29.4	Unbiased	FG errors
proton	47.2	Unbiased	FG errors
proton	60.9	Unbiased	FG errors
proton	101.4	Unbiased	FG errors
proton	151.2	Unbiased	FG errors
proton	200	Unbiased	FG errors
proton	29.4	E/R/P/R	SEFIs
proton	47.2	E/R/P/R	SEFIs
proton	60.9	E/R/P/R	SEFIs
proton	101.4	E/R/P/R	SEFIs
proton	151.2	E/R/P/R	SEFIs
proton	200	E/R/P/R	SEFIs

Table 4: Proton beams and test conditions used at PIF.

Proton irradiations were performed at the Proton Irradiation Facility (PIF) in Villigen, Switzerland, using the beams listed in **Table 4.**

The test setup for heavy ions consists of an FPGA motherboard controlled by a host PC and a daughterboard with an open-top socket, where the DUT is placed The only difference with the TID setup described in Section 4.1 is that for heavy-ion tests there is no need for the relatively long cables between the FPGA board and the daughterboard. The test setup for protons is virtually identical to the one used for total dose tests.

Both biased and unbiased conditions were used during heavy-ion and proton irradiations.

For the biased tests, the samples were exercised in different operating modes:

- Standby with active chip enable (to detect possible current spikes and/or destructive events) (only heavy ions)
- Erase/Read/Program/Read (E/R/P/R) loops (to detect SEFIs)

After each erase, program, and read operation during the E/R/P/R loops, different parameters were monitored under irradiation (see total dose section for further details). In particular:

- After erase operations we logged:
  - SR, to detect erase fails;
  - RB low time, to measure the erase time;
- After each program operation we logged:
  - SR, to detect program fails;
  - RB low time, to measure the program time;
- After each read operation we logged:
  - RB low time, to measure the read time;
  - Number and location of errors.

For the unbiased tests, the memories were exposed unbiased and programmed and read out of the beam.

Overall, 3 MLC NAND Flash memories were measured under heavy-ion irradiation, one with the high-LET cocktail and another one with the high-energy cocktail; 2 devices were measured under proton irradiation.

5.2 Experimental Results

Floating gate errors and SEFIs were observed both with heavy ions and protons, whereas the devices did not exhibit any latchup.

5.2.1 Floating Gate Errors

Floating Gate (FG) errors induced by heavy ions were measured with the device unbiased, with both normal and tilted irradiations. The FG error cross sections per bit for each program level are illustrated in **Fig. 13**, as a function of the effective LET, for the high energy cocktail. Program levels are labeled '11', '01', '00', '10'. Error bars are smaller than the symbols in **Fig. 13.** The heavy-ion cross section curve has been fitted with a Weibull function, independent from the program level, having the following parameters:

threshold LET: L_0=0.35 MeV·mg^{-1}·cm^2
width: W =50 MeV·mg^{-1}·cm^2
exponent: s=1.3,
saturation: A=6·10^{-10} cm^2

Errors induced by protons have been measured with the device unbiased. The FG error cross section per bit as a function of energy after proton irradiation is illustrated in **Fig. 14**.

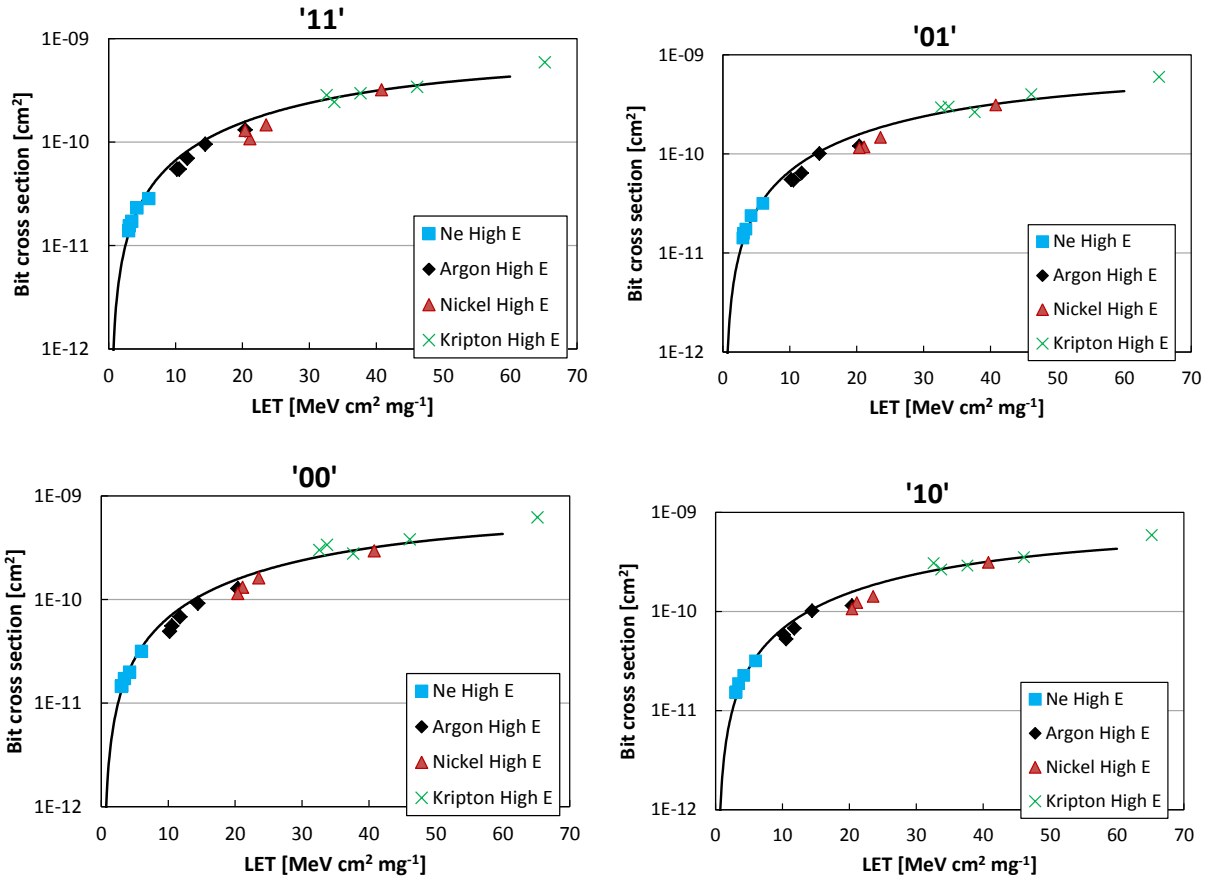

Figure 13: Heavy-ion Induced Floating Gate Errors Bit Cross Section for each program level. (MG39 used for Ne, Argon and Nickel, MG40 for Kripton).

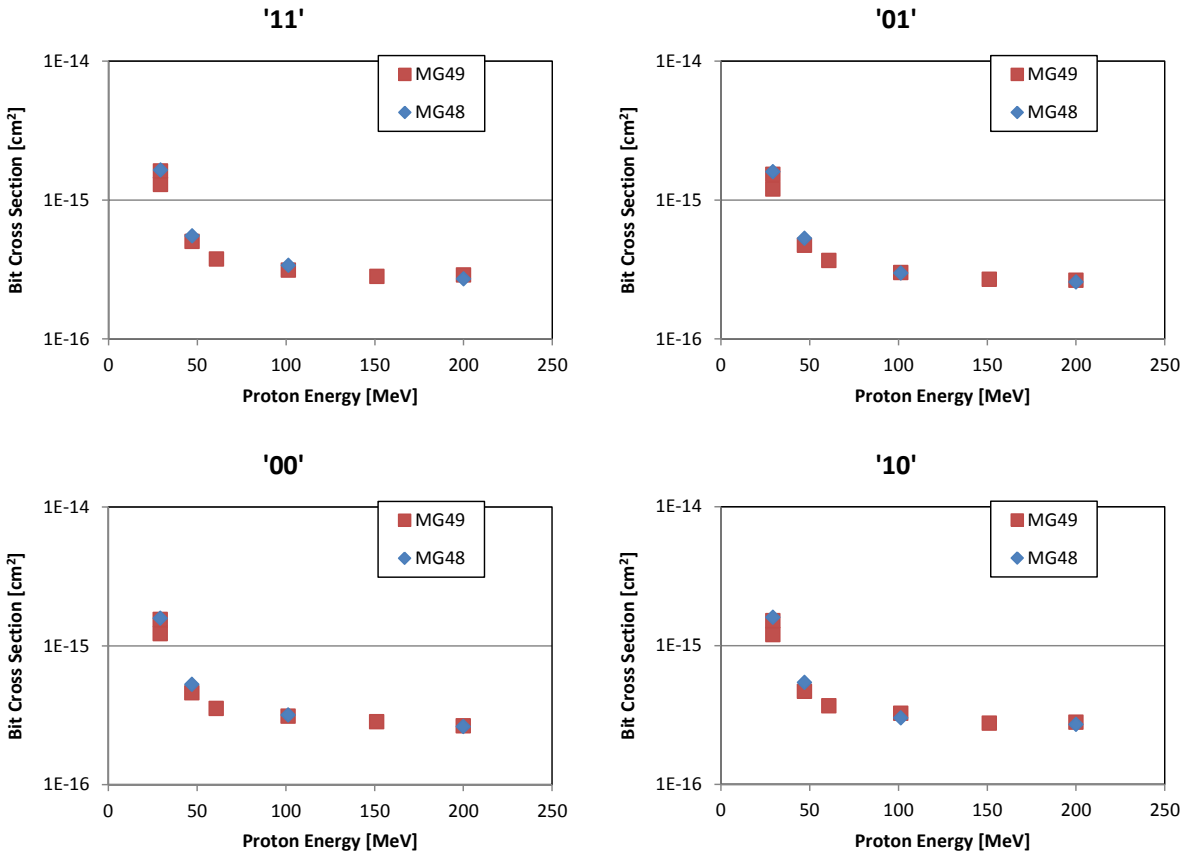

Figure 14: Proton Induced Floating Gate Errors Bit Cross Section for each program level.

5.2.2 SEFIs

Single Event Functional Interrupts (SEFI) were measured with the devices irradiated at normal incidence, during repeated Erase/Read/Program/Read (ERPR) loops. **Fig. 15** shows the device SEFI cross section versus ion LET, measured with the HIF high LET cocktail. Poisson error bars are also reported in **Fig. 15**.

The heavy-ion cross section curve has been fitted with a Weibull function having the following parameters:

threshold LET: L_0=2.85 MeV·mg^{-1}·cm^2
width: W =22 MeV·mg^{-1}·cm^2
exponent: s=2
saturation: A=1.13·10^{-4} cm^2

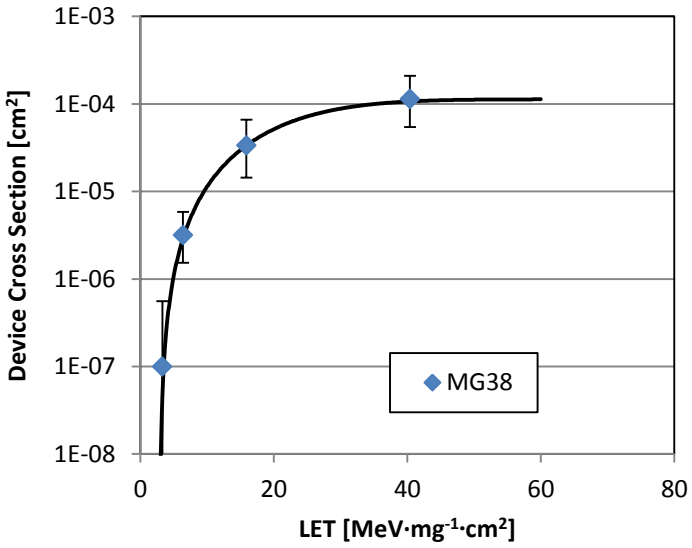

Figure 15: SEFI device Cross Section as a function of LET with heavy-ion irradiation (errors bars are at 95% confidence interval).

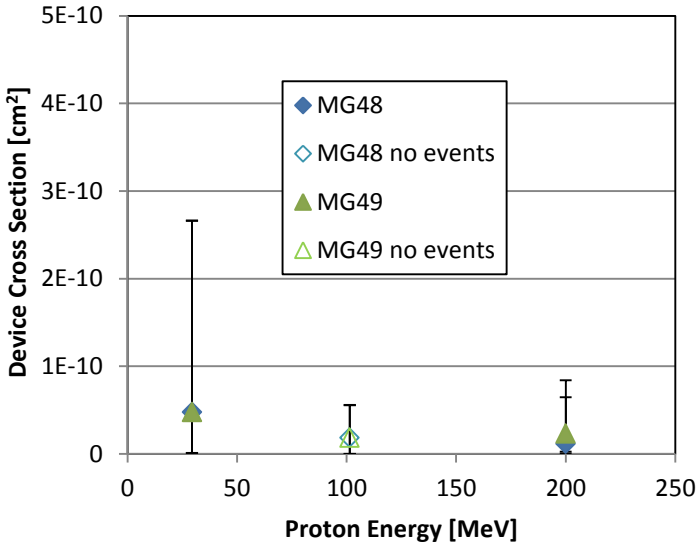

Figure 16: SEFI device Cross Section as a function of LET with proton irradiation (errors bars are at 95% confidence interval. When no errors are recorded, empty symbols indicate minimum measurable

SEFIs were also observed with protons, although the number of events is much smaller, hence the determination of the cross section is less accurate. **Fig.16** shows the results as a function of proton energy with Poisson error bars.

5.3 Error-rate Calculations

Creme96 has been used to calculate error rates in the following three orbits:

1) International Space Station (ISS) orbit

2) PROBA II orbit (LEO, perigee: 715.2 km, apogee: 735.1 km, inclination: 98.3°)

3) Geosynchronous orbit.

Solar minimum, worst-day flare and peak 5 min flare have been used for the calculations.

Table 5 reports the results of error rate calculations. The depth of the sensitive volume is set to 100 nm for floating gate errors (i.e., the thickness of the floating gate). The floating gate error rates are calculated without ECC. A single node with a 2μm thickness is used to calculate SEFI rates.

Orbit	ISS 51.6° 500 km	ISS 51.6° 500 km	ISS 51.6° 500 km	PROBA II 98.3° 715-735 km	PROBA II 98.3° 715-735 km	PROBA II 98.3° 715-735 km	GEO	GEO	GEO
Trapped protons	AP8min, avg flux			AP8min, avg flux					
Magnetic weather condition	quiet	quiet	quiet	quiet	quiet	quiet			
Solar conditions	solar min	flare, worst-day	flare, peak 5 minutes	solar min	flare, worst-day	flare, peak 5 minutes	solar min	flare, worst-day	flare, peak 5 minutes
Shielding	100 mils Al	100 mils Al	100 mils Al	100 mils Al	100 mils Al	100 mils Al	100 mils Al	100 mils Al	100 mils Al
Heavy-ion errors on programmed FG [$bit^{-1} \cdot s^{-1}$]	2.28E-15	6.27E-13	2.32E-12	6.00E-15	5.37E-12	2.00E-11	1.95E-14	2.57E-11	9.63E-11
Proton errors on programmed FG [$bit^{-1} \cdot s^{-1}$]	1.16E-14	1.29E-13	4.72E-13	3.51E-14	2.48E-12	9.06E-12	1.24E-15	1.31E-11	4.80E-11
Heavy-ion SEFIs [s^{-1}]	2.72E-10	1.04E-07	3.83E-07	8.02E-10	7.72E-07	2.87E-06	2.78E-09	3.59E-06	1.34E-05
Proton SEFIs [s^{-1}]	6.79E-10	7.02E-09	2.56E-08	2.02E-09	1.25E-07	4.57E-07	5.42E-11	6.60E-07	2.41E-06

Table 5: Error rate calculations.

Raw bit error rate	Uncorrectable bit error rate
0.000001	1.85E-81
1.00E-05	1.72E-56
1.00E-04	8.15E-32
1.00E-03	5E-10

Table 6: Uncorrectable bit error rate as a function of raw bit error rate, using a 24-bit ECC per 1080 bytes, as specified by the manufacturer.

The manufacturer specifies an ECC capable of correcting 24 bits per codeword of 1080 bytes. **Table 6** can be used to estimate the uncorrectable error rate from the raw bit error rate, using the ECC specified by the manufacturer. In turn, the raw bit error rate is obtained by multiplying the rates in **Table 5** by the amount of time the memory has been exposed since the last write (ECC must cope with the number of errors accumulated since the last refresh or write).

6 Conclusions

Table 7 summarizes the effects observed in the tested NAND MLC samples during TID irradiations with devices in different operating conditions. The average dose at which those effects first appeared is indicated for both gamma and x-ray irradiations.

Table 8 and **Table 9** show a summary for the events observed in the tested NAND MLC samples during heavy-ion and proton irradiation, respectively. As seen in **Table 8**, both FG errors and SEFIs were observed starting from LET values of 3 MeV cm^2/mg (the lowest used LET). The saturation cross section for FG errors is in the order of 10^{-10} cm^2. FG errors and SEFIs were observed with all tested proton energies (**Table 9**).

Observed effect	**Memory operating condition**	**Av. gamma failure dose [krad(Si)]**	**Av. x-ray failure dose [krad(Si)]**
Retention errors (in 1% of the tested cells)	High-duty cycle, cells in retention without refresh	22	26
	Low-duty cycle, cells in retention with refresh	52	-
	Unbiased, cells in retention without refresh	22	-
Failure of erase operation during E/R/P/R loops	High-duty cycle E/R/P/R loops	50	57
	Low-duty cycle E/R/P/R loops	70	-
	Unbiased	68	-
Errors after erase (in 10% of the tested cells)	High-duty cycle E/R/P/R loops	68	86
	Low-duty cycle E/R/P/R loops	106	-
	Unbiased	69	-
Failure of program operation during E/R/P/R loops	High-duty cycle E/R/P/R loops	61	62
	Low-duty cycle E/R/P/R loops	69	-
	Unbiased	69	-
Errors after program (in 10% of the tested cells)	High-duty cycle E/R/P/R loops	66	60
	Low-duty cycle E/R/P/R loops	58	-
	Unbiased	69	-

Table 7: Summary of the observed effects during TID irradiations.

Observed effect	**Operating condition**	**Threshold LET [MeV cm^2/mg]**	**Saturation σ [cm^2]**
Floating Gate cell errors	Unbiased	< 3	~ 6E-10 per bit
SEFIs	E/R/P/R loops	< 3	~ 1E-4 per device

Table 8: Summary of the observed effects during during heavy-ion irradiations.

Observed effect	**Operating condition**	**Threshold Energy [MeV]**	**Max σ [cm^2]**
Floating Gate cell errors	Unbiased	< 29.4	~ 2E-15 per bit
SEFIs	E/R/P/R loops	< 29.4	~ 1E-10 per device

Table 9: Summary of the observed effects during proton irradiations.